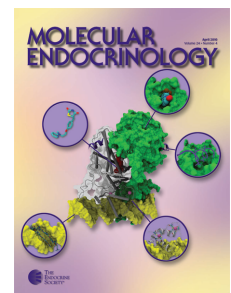# Endocrinology

17²-Estradiol at Physiological Concentrations Augments Ca2+-Activated K+ Currents via Estrogen Receptor ² in the Gonadotropin-Releasing Hormone Neuronal Cell Line GT1-7

Ichiro Nishimura, Kumiko Ui-Tei, Kaoru Saigo, Hirotaka Ishii, Yasuo Sakuma and Masakatsu Kato

17β-Estradiol at Physiological Concentrations Augments Ca²⁺-Activated K⁺ Currents via Estrogen Receptor β in the Gonadotropin-Releasing Hormone Neuronal Cell Line GT1-7

Ichiro Nishimura, Kumiko Ui-Tei, Kaoru Saigo, Hirotaka Ishii, Yasuo Sakuma, and Masakatsu Kato

Department of Physiology (I.N., H.I., Y.S., M.K.), Nippon Medical School, Tokyo 113-8602, Japan; and Department of Biophysics and Biochemistry (K.U.-T., K.S.), School of Science, University of Tokyo, Tokyo 113-0033, Japan

Estrogens play essential roles in the neuroendocrine control of reproduction. In the present study, we focused on the effects of 17β-estradiol (E2) on the K⁺ currents that regulate neuronal cell excitability and carried out perforated patch-clamp experiments with the GnRH-secreting neuronal cell line GT1-7. We revealed that a 3-d incubation with E2 at physiological concentrations (100 pm to 1 nm) augmented Ca²⁺-activated K⁺ [K(Ca)] currents without influencing Ca²⁺-insensitive voltage-gated K⁺ currents in GT1-7 cells. Acute application of E2 (1 nm) had no effect on the either type of K⁺ current. The augmentation was completely blocked by an estrogen receptor (ER) antagonist, ICI-182,780. An ERβ-selec-

tive agonist, 2,3-bis(4-hydroxyphenyl)-propionitrile, augmented the K(Ca) currents, although an ERα-selective agonist, 4,4′,4″-[4-propyl-(1H)-pyrazole-1,3,5-triyl]tris-phenol, had no effect. Knockdown of ERβ by means of RNA interference blocked the effect of E2 on the K(Ca) currents. Furthermore, semiquantitative RT-PCR analysis revealed that the levels of BK channel subunit mRNAs for α and β4 were significantly increased by incubating cells with 300 pm E2 for 3 d. In conclusion, E2 at physiological concentrations augments K(Ca) currents through ERβ in the GT1-7 GnRH neuronal cell line and increases the expression of the BK channel subunit mRNAs, α and β4. (*Endocrinology* 149: 774–782, 2008)

THE GnRH NEUROSECRETORY system constitutes the final common pathway in the central regulation of reproduction. For the normal functioning of this system, the steroid hormone 17β-estradiol (E2) is indispensable. Despite the importance of E2 in this system, its mechanisms of action are largely unknown (1). E2 acts either through two subtypes of nuclear estrogen receptors (ERs), ERα and ERβ, or directly on membrane proteins, including a hypothetical membrane ER (2). Modulation of K⁺ channels by E2 has been reported. E2 hyperpolarizes neurons of the medial amygdala (3) and preoptic area (4) by increasing their K⁺ permeability and depolarizes hypothalamic neurons by decreasing K⁺ permeability (5). E2 rapidly alters the firing patterns of primate GnRH neurons in culture (6). The acute application of E2 increases the inward currents and decreases the outward currents of hypothalamic neurons (7). E2 acutely modulates the function of large-conductance Ca²⁺- and voltage-activated K⁺ (BK) channels either through a cGMP-dependent mechanism, as in coronary artery endothelial cells (8), or by binding to the auxiliary β1-subunit of BK channels, as in the

oocyte expression system (9). These actions are considered to be nongenomic and appear only at nanomolar to micromolar concentrations of E2, which exceed the concentrations of rodent plasma E2 (10^{-11} to 10^{-10} m) (10, 11). In addition, implantation of E2 pellets in ovariectomized mice decreased both the delayed rectifier K⁺ and A currents in GnRH neurons (12), suggesting a long-term effect of E2.

An immortalized GnRH-secreting neuronal cell line, GT1, generated by genetically targeted tumorigenesis in transgenic mice, is thought to preserve many of the characteristics of native GnRH neurons (13). These neurons generate spontaneous action potentials, exhibit transient oscillations in intracellular Ca²⁺ concentration (14, 15), and secrete GnRH in a pulsatile manner (16, 17). Moreover, GT1-7 cells exhibit K⁺ currents, including delayed rectifier K⁺ currents, A currents, inward rectifier K⁺ currents, BK currents (18, 19), and small-conductance Ca²⁺-activated K⁺ (SK) currents (20) and express both ERα and ERβ (21, 22). In addition, E2 directly represses GnRH gene expression in GT1-7 cells (22). Thus, this cell line is suitable for studying the action of estrogens on K⁺ channels. In the present study, we analyzed the action of E2 on the function of K⁺ channels and found that Ca²⁺-activated K⁺ [K(Ca)] currents are positively modulated by physiological concentrations of E2 via ERβ. No acute effects of E2 on K(Ca) currents were observed at physiological concentrations.

Materials and Methods

Cell culture

GT1-7 cells (provided by Dr. R. Weiner, University of California, San Francisco) were cultured in DMEM (without phenol red; Irvine Scien-

tific, Santa Ana, CA) supplemented with 1 mM sodium pyruvate, 24 mM NaHCO$_3$, 4 mM L-glutamine, 10% fetal bovine serum (JRH Biosciences, Lenexa, KS), 100 U/ml penicillin, and 0.1 mg/ml streptomycin (Invitrogen, Carlsbad, CA). The fetal bovine serum contained 72 pM E2; therefore, the concentration of E2 in the culture media without E2 supplementation was 7.2 pM. The cultures were maintained at 37 C in a water-saturated atmosphere of 95% air and 5% CO$_2$. The culture medium was changed every 3–4 d, and the cells were passaged every 1–2 wk and used in experiments within 10 passages. For electrophysiological experiments, the cells were plated onto poly-L-lysine-coated coverslips and cultured for 3 d with or without selective ER modulators.

Treatment of cells with E2 and ER modulators

Cells were incubated with E2 (10 pM to 10 nM) for 3 d. The effect of the ER antagonist ICI-182,780 (ICI) was determined by incubating cells in medium containing ICI (0.3–10 µM) and E2 (300 pM) for 3 d. 4,4′,4″-[4-Propyl-(1H)-pyrazole-1,3,5-triyl]tris-phenol (PPT) was used as an ERα-selective agonist and 2,3-bis(4-hydroxyphenyl)-propionitrile (DPN) was used as an ERβ-selective agonist. Cells were incubated with PPT (1–10 nM) or DPN (0.1–10 nM) for 3 d to determine the effects of these agonists.

RNA interference

Using Lipofectamine 2000 (Invitrogen), GT1-7 cells were cotransfected with pCAGIPuro-EGFP (0.3 µg/ml), encoding enhanced green fluorescent protein and puromycin-resistance genes, and 50 nM small interfering RNA (siRNA) against either mouse ERα or ERβ, according to the manufacturer's protocol. The sequences of the siRNAs were designed according to the guidelines reported by Ui-Tei *et al.* (23): 5′-CUGGUUCAUAUGAUCAACUGG-3′ for sense ERα siRNA (1146S); 3′-AGUUGAUCAUAUGAACCAGCU-5′ for antisense ERα siRNA (1146A); 5′-GGAACUGGUGCACAUGAUUGG-3′ for sense ERβ siRNA (775S); and 3′-AAUCAUGUGCACCAGUUCCUU-5′ for antisense ERβ siRNA (775A). After siRNA transfection, we prepared the cells for each set of experiments according to the following procedures. For electrophysiological experiments, cells were incubated with E2 for 3 d after overnight preincubation without E2. For RT-PCR, the cells were incubated with puromycin (1 µg/ml) for 2 d to isolate transfected cells after overnight preincubation without E2 and puromycin.

RT-PCR

Total RNA was extracted from GT1-7 cells using RNeasy Mini kits (QIAGEN, Valencia, CA) following the manufacturer's instructions. Total RNA was then treated with 5 U RNase-free DNase I (Ambion, Austin, TX). The concentration of total RNA was quantified by measurement of the absorption at 260 nm. Total RNA was reverse-transcribed into first-strand cDNA using an oligo-dT primer. Reaction mixtures (final volume, 25 µl) contained 5 µg total RNA, 1× RT buffer, 1 mM dNTP mixture, 1 µg oligo-(dT)$_{15}$ primer (Promega, Madison, WI), 20 U RNasin *Plus*, (Promega), and 100 U Maloney murine leukemia virus reverse transcriptase (ReverTra Ace; Toyobo Bio, Osaka, Japan). The reaction was carried out at 42 C for 1 h and stopped by heating at 72 C for 15 min. cDNA was treated with 4 U RNase H (Takara Bio, Shiga, Japan) at 37 C for 30 min and stored at −20 C.

PCR was performed in a 20-µl reaction mixture comprising cDNA corresponding to 50 ng total RNA, 1× PCR buffer, 0.2 mM dNTP mixture, 0.2 µM forward and reverse primers, and 0.63 U Blend *Taq plus* (Toyobo Bio). The PCR conditions were 94 C for 2 min, followed by 18–38 cycles of 94 C for 30 sec, a suitable temperature for each primer pair for 20 sec, 72 C for 30 sec, and finally, 72 C for 5 min. The sequences of oligonucleotide primers used in this study are listed in Table 1. To avoid amplifying any contaminating genomic DNA, the primer pairs were designed from different exons. The optimal number of PCR cycles was determined over a range of cycles to identify an exponentially linear range of amplification for each transcript extracted from GT1-7 cells. PCR products (5 µl) were separated by electrophoresis on 2% agarose gels and visualized by ethidium bromide staining under UV irradiation. Gel images were captured using a FAS-III system (Toyobo Bio).

Semiquantitative RT-PCR

The expression levels of BK channel subunit mRNAs in GT1-7 cells incubated with or without E2 were measured by semiquantitative RT-PCR. Total RNA was extracted from GT1-7 cells incubated for 3 d without E2 for the control group and with 300 pM E2 for the experimental group. RT-PCR was performed using the same method as described above. The number of PCR cycles was selected to be within the range of the linear amplification for each transcript: 16 cycles for GAPDH, 26 cycles for Kcnma1 (α), 25 cycles for Kcnmb1 (β1), 23 cycles for Kcnmb2 (β2), and 23 cycles for Kcnmb4 (β4). A quantitative densitometry anal-

TABLE 1. Sequences of the primers employed for RT-PCR amplifications, amplicon length, annealing temperatures, and PCR cycles

Gene name	Primer sequence (5′–3′)	Amplicon length (bp)	Annealing temperature (C)	PCR cycles
ERα		404	59	28
Forward	TGGCTGGAGATTCTGATGATTGGT			
Reverse	ATGTGCCGGATATGGGAAAGAA			
ERβ		586	65	38
Forward	CTTTGACATGCTCCTGGCGACGAC			
Reverse	GGGAAGCGCAACGTGGGTAAGG			
GAPDH		359	62	18
Forward	TGAAGGTCGGTGTGAACGGATTTG			
Reverse	GGCGGAGATGATGACCCTTTTG			
Kcnma1		537	58	30
Forward	CGCCAGCCGTCCATCACA			
Reverse	CAGCCGGTAAATTCCAAAACAAAG			
Kcnmb1		331	61	28
Forward	CAGTGGCCATGGGGAAGAAGC			
Reverse	CTGGGGATATAGGAGCACTGTTGGTTT			
Kcnmb2		625	66	26
Forward	CCAGTGGCCGGACCTCTTCATCTTACAG			
Reverse	ATTGCCACACCCCCAGCCATCATAC			
Kcnmb3		222	67	35
Forward	GATCCCCATGCCTGCAGGTGTTCGTAAA			
Reverse	CCAAGGGGCCATCGGGACTGTAGA			
Kcnmb4		589	63	26
Forward	CTCCGGCATCCTGTCGCTCTTCA			
Reverse	GGTCTCGGCTTCCCACAATCCTC			

ysis was performed using CS analyzer software (Atto Corp., Tokyo, Japan). The levels of mRNAs for BK channel subunits in each sample were expressed as a ratio to the level of GAPDH in the same sample. Values were normalized to control levels.

DNA sequencing

PCR products were extracted from agarose gels using a Wizard SV Gel and PCR Clean-up system (Promega), and cloned into pGEM-T-Easy vectors (Promega). Sequencing reactions were performed using a Big-Dye Terminator version 3.1 Cycle sequencing kit (Applied Biosystems, Foster City, CA). Fluorescent signals were detected using an ABI PRISM 310 Genetic Analyzer (Applied Biosystems).

Electrophysiology

A List EPC-9 patch-clamp system (HEKA Elektronik, Lambrecht, Germany) was used for recordings and data analyses. Whole-cell currents were recorded using a perforated patch-clamp configuration with 50 μg/ml amphotericin B (Seikagaku Corp, Tokyo, Japan) (24, 25) at room temperature (25 C). The patch electrodes were made of borosilicate glass capillaries and had a resistance of 5–10 MΩ. The indifferent electrode consisted of an Ag-AgCl wire connected to the bath solution via an agar bridge. For the recording of K$^+$ currents, the pipette solution consisted of 95 mM K-aspartate, 47.5 mM KCl, 1 mM MgCl$_2$, 0.1 mM EGTA, 10 mM HEPES, and 2 mM ATP-Mg (pH 7.2; osmolality, 270 mOsm). The extracellular solution consisted of 137.5 mM NaCl, 5 mM KCl, 2.5 mM CaCl$_2$, 0.8 mM MgCl$_2$, 10 mM glucose, 20 mM HEPES, and 0.6 mM NaHCO$_3$ (pH 7.4; osmolality, 300 mOsm). Na$^+$ currents were blocked by 0.3 μM tetrodotoxin (Sankyo Co., Ltd., Tokyo, Japan). The difference in the osmolality between the pipette solution and extracellular solution somehow helped to form a stable giga-seal in the perforated patch configuration. For the recording of Ca^{2+} currents, K$^+$ in the pipette solution was replaced with Cs$^+$. The extracellular solution consisted of 106.5 mM NaCl, 5 mM CsCl, 0.8 mM MgCl$_2$, 10 mM CaCl$_2$, 10 mM glucose, 20 mM HEPES, 0.6 mM NaHCO$_3$, and 10 mM tetraethylammonium chloride (pH 7.4; osmolality, 300 mOsm). Na$^+$ currents were blocked by 0.3 μM tetrodotoxin.

The currents were filtered at 2.3 kHz, digitized at 10 kHz, and recorded. Data were collected only when the series resistance was stable and less than 25 MΩ. Up to 70% of the series resistance was electronically compensated. Capacitive and leak currents were subtracted by means of the P/4 protocol. Cell capacitance was 9.0 $\pm$ 0.2 pF (mean $\pm$ SEM, n = 166). The liquid junction potential was not compensated. K$^+$ currents were activated by 50-msec voltage steps from -60 to $+60$ mV in 10-mV increments from a holding potential of -90 mV at 0.2 Hz (Fig. 1A). The K$^+$ current values were determined as the means for the last 2.5 msec of the voltage pulse. After-hyperpolarization currents (I$_{AHP}$) were activated by a voltage protocol comprising a 100-msec voltage pulse to $+30$ mV from a holding potential of -90 mV, followed by a 5-sec voltage step to -50 mV. The voltage pulse was applied every 30 sec (Fig. 4C). Ca^{2+} currents were activated by 100-msec voltage steps from -60 to $+60$ mV in 10-mV increments from a holding potential of -100 mV at 0.2 Hz (Fig. 5A). The peak Ca^{2+} currents were determined for the analysis.

Chemicals

SNX-482, charybdotoxin (ChTX), and apamin were purchased from the Peptide Institute (Osaka, Japan). Nifedipine was purchased from Sigma. ICI, PPT, and DPN were purchased from Tocris (Ellisville, MO). All drugs were prepared immediately before use.

Statistical analysis

Data are presented as the means $\pm$ SEM. The differences were analyzed by a one-way ANOVA followed by the Tukey-Kramer multiple comparison test, Wilcoxon signed-rank test, or *t* test. $P < 0.05$ was considered statistically significant.

Results

K(Ca) currents and Ca^{2+} currents

The activation of the K$^+$ currents started at -10 mV, and the amplitudes increased with depolarization (Fig. 1B). The
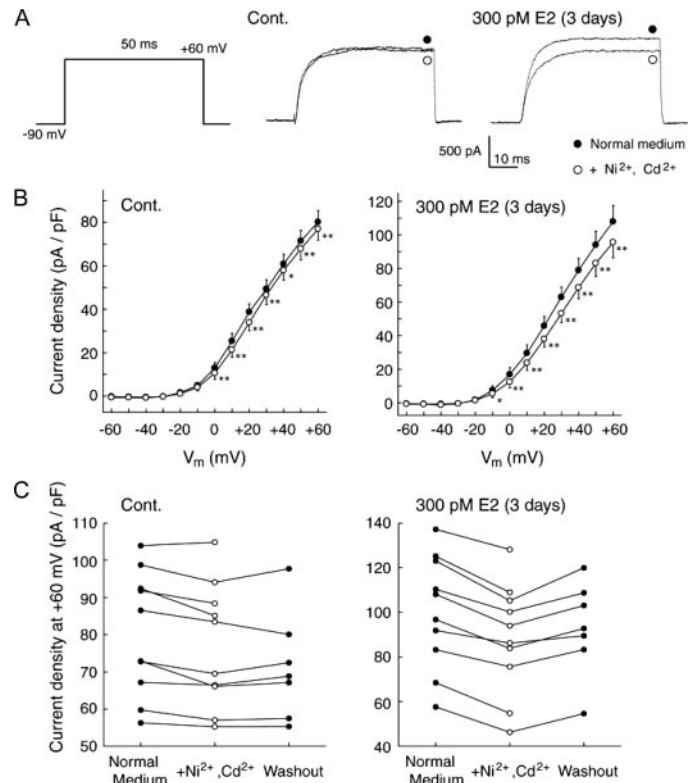

FIG. 1. K(Ca) currents and Ca^{2+}-insensitive K$^+$ currents in GT1-7 cells. The K$^+$ currents were activated by 50-msec voltage pulses (-60 to $+60$ mV in 10-mV increments) from a holding potential of -90 mV. A, The voltage protocol and current traces activated by voltage pulse to $+60$ mV are shown. Under the control conditions, Ni^{2+} (100 μM) and Cd^{2+} (200 μM) slightly reduced the K$^+$ currents. However, Ni^{2+} and Cd^{2+} clearly reduced the currents in cells incubated with 300 pM E2 for 3 d. B, The effects of Ni^{2+} and Cd^{2+} are collectively shown in the current-voltage relationship of the K$^+$ currents in the control cells (n = 10) and in the cells incubated with 300 pM E2 for 3 d (n = 10). C, The effects of Ni^{2+} and Cd^{2+} and washout are shown for individual cells. Three cells were lost during the washout. Therefore, only seven data points for washout are shown. *, $P < 0.05$ *vs.* normal medium; **, $P < 0.01$ *vs.* normal medium using the Wilcoxon signed-rank test.

K$^+$ currents were slightly reduced by the addition of Ni^{2+} (NiCl$_2$; 100 μM) and Cd^{2+} (CdCl$_2$; 200 μM), which completely block Ca^{2+} channels. Ni^{2+} and Cd^{2+} clearly reduced the amplitude of the K$^+$ currents in cells incubated with 300 pM E2 for 3 d. The effects of Ni^{2+} and Cd^{2+} were almost completely abolished on washout (Fig. 1C). The rates of recovery from the maximal amplitude were 97.2 $\pm$ 1.4% in control cells and 97.4 $\pm$ 0.8% in cells incubated with 300 pM E2. These Ni^{2+}- and Cd^{2+}-blockable K$^+$ currents are referred to as the K(Ca) currents, and the remaining currents are referred to as the Ca^{2+}-insensitive K$^+$ currents. The K(Ca) currents were not augmented by a 1-d incubation with E2 (data not shown). Acute application (5 min) of 1 nM E2 had no effect on the total K$^+$ currents in the cell groups incubated with or without 300 pM E2 for 3 d (data not shown).

To determine the concentration-response relationship of E2, incubations were carried out with 10 pM to 10 nM E2 for 3 d. E2 had no effect on the Ca^{2+}-insensitive K$^+$ currents (Fig. 2), whereas it augmented the K(Ca) currents in the concentration range of 100 pM to 1 nM (Fig. 3). The EC$_{50}$ was 56.5
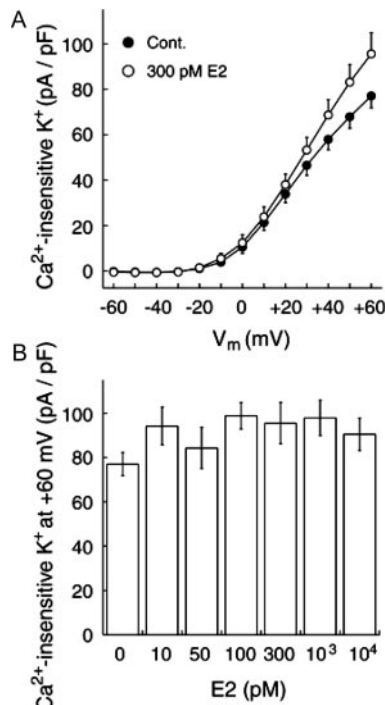
FIG. 2. E2 had no effect on the Ca^{2+}-insensitive K^+ currents, which are the remaining currents after application of Ni^{2+} and Cd^{2+}. A, The current-voltage relationships of the Ca^{2+}-insensitive K^+ currents are shown for GT1-7 cells incubated with 300 pM E2 ($\bigcirc$, n = 10) and without 300 pM E2 ($\bullet$, n = 10). The data are repeated from Fig. 1B. B, Concentration-response relationship of E2 on the Ca^{2+}-insensitive K^+ currents at +60 mV (n = 7–10).

FIG. 3. Effect of E2 on the K(Ca) currents. The K(Ca) currents were obtained by subtracting the Ni^{2+}- and Cd^{2+}-insensitive currents from the total K^+ currents. Cells were incubated with E2 for 3 d. A, Current-voltage relationships of the K(Ca) currents in the control cells ($\bullet$, n = 10) and in the cells incubated with 300 pM E2 for 3 d ($\bigcirc$, n = 10). E2 (300 pM) augmented K(Ca) currents at +30 to +60 mV. B, Concentration-response relationship of E2 on K(Ca) currents (n = 7–10). E2 had no effect on the K(Ca) currents activated at +20 mV. It is to be noted that the maximal amplitude of voltage-gated Ca^{2+} currents is attained around this voltage. The K(Ca) currents activated at +60 mV were clearly augmented by physiological concentrations of E2. However, 10 nM E2 had no statistically significant effect on the K(Ca) currents. There was no statistically significant difference between the current in cells incubated with 1 nM E2 and that with 10 nM E2. **, $P < 0.01$ *vs.* control (0 pM E2) using the Tukey-Kramer multiple comparison test.

pM. The effects of E2 were observed at +30 mV to +60 mV but not at potentials more negative than +30 mV (Fig. 3A). In control cells, the K(Ca) currents were 4.8 ± 0.5 pA/pF at +20 mV and 3.3 ± 0.8 pA/pF at +60 mV. It is to be noted that the currents from the control cells were not increased at potentials more positive than +20 mV. In cells incubated with 300 pM E2, the K(Ca) currents were 7.7 ± 1.5 pA/pF at +20 mV and 12.3 ± 1.2 pA/pF at +60 mV. A BK channel blocker, ChTX (100 nM), slightly reduced the K^+ currents in control cells and clearly reduced those in cells incubated with 300 pM E2 (Fig. 4, A and B). This inhibitory effect by ChTX was not observed when Ni^{2+} and Cd^{2+} were applied before ChTX (data not shown). The ChTX-sensitive component comprised 80.1 ± 7.8% of the K(Ca) currents in control cells and 70.1 ± 5.7% of the K(Ca) currents in cells incubated with E2 (Fig. 4B). On the other hand, the SK channel blocker apamin (100 nM) did not reduce the K^+ currents at +60 mV in cells incubated with 300 pM E2 (Fig. 4B). Furthermore, I_{AHP} were hardly observed in cells incubated with or without 300 pM E2 (Fig. 4C).

In addition to the K(Ca) currents, the voltage-gated Ca^{2+} currents were examined in the presence of 10 mM Ca^{2+} in the extracellular solution. The maximal amplitude was observed at around +20 mV in GT1-7 cells (Fig. 5A). Ca^{2+} currents at +20 mV were −19.3 ± 3.0 pA/pF in control cells and −25.9 ± 4.3 pA/pF in cells incubated with 300 pM E2 for 3 d (Fig. 5B). There was no statistically significant effect of E2 on the Ca^{2+} currents. Simultaneous application of Ni^{2+} (100 μM) and
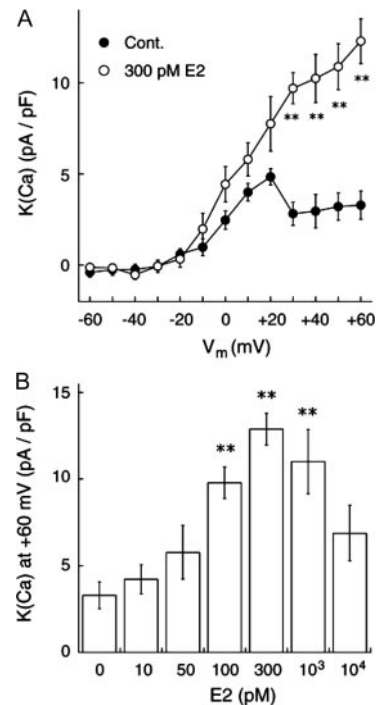
Cd^{2+} (200 μM) completely blocked the Ca^{2+} currents (Fig. 5, A and B). Pharmacological dissection with specific blockers determined the diversity of voltage-gated Ca^{2+} channel subtypes in GT1-7 cells. The R-type Ca^{2+} channel blocker SNX-486 (100 nM), the L-type Ca^{2+} channel blocker nifedipine (10 μM), and the T-type Ca^{2+} channel blocker Ni^{2+} (100 μM) were used. SNX-486, nifedipine, and Ni^{2+} inhibited the Ca^{2+} currents by 72.2 ± 3.6, 10.2 ± 2.3, and 3.3 ± 1.1%, respectively, in control cells (n = 10), and by 77.5 ± 2.2, 8.5 ± 1.7, and 4.9 ± 1.4%, respectively, in cells incubated with 300 pM E2 for 3 d (n = 10).

Effects of ER agonists and antagonist

To determine whether E2 acts through ERs, an ER antagonist, ICI, was added to the culture medium with 300 pM E2. ICI blocked the effect of E2 on K(Ca) currents in a concentration-dependent manner, with an IC_{50} of 1.2 μM (Fig. 6). To examine whether E2 affected either ERα or ERβ, a selective agonist for each subtype of ER was used. The selective agonist for ERβ (DPN) augmented the K(Ca) currents, whereas that for ERα (PPT) had no effect on K(Ca) currents (Fig. 7A).
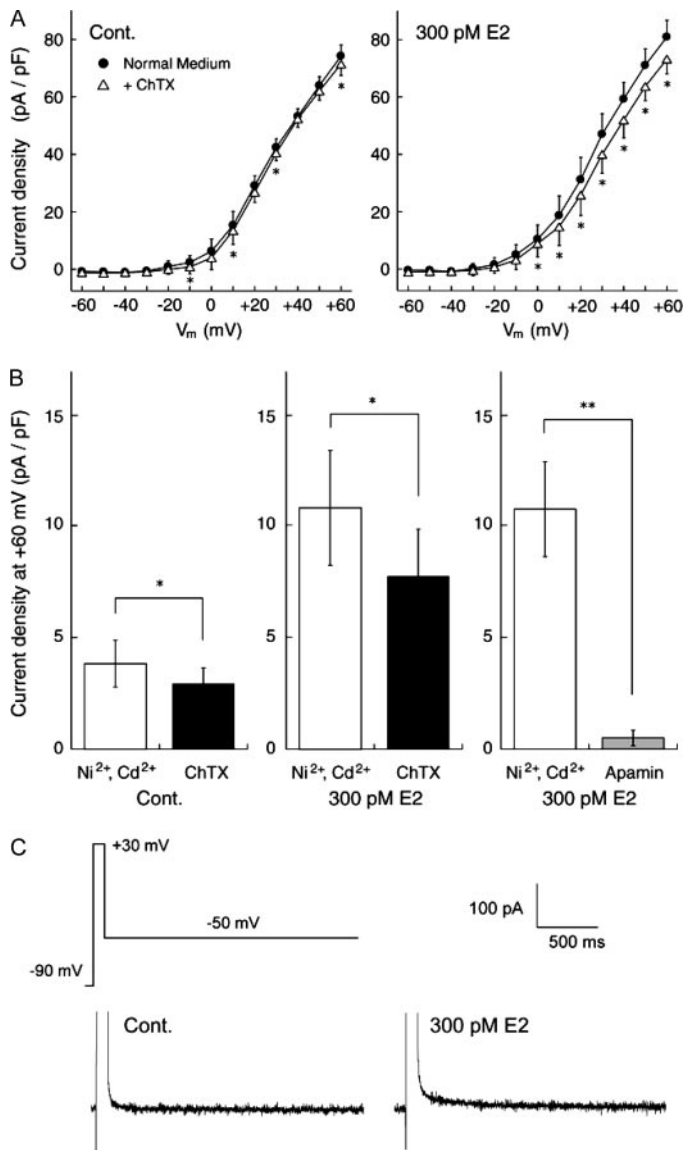
FIG. 4. The K(Ca) channel blocker ChTX reduced the K^+ currents. A, Current-voltage relationships of the K^+ currents in control (n = 7) and 300 pM E2-treated cells (n = 7) are shown. K^+ currents were evoked by voltage steps from −60 to +60 mV in 10-mV increments from a holding potential of −90 mV. Data for Ni^{2+} and Cd^{2+} are not shown for clarity. B, ChTX (100 nM)-sensitive currents (*black bars*), Ni^{2+} (100 μM)- and Cd^{2+} (200 μM)-sensitive currents [*white bars*, K(Ca) currents] and apamin-sensitive currents (*gray bar*) are shown. Approximately 80% of the K(Ca) currents were ChTX sensitive in control cells (n = 7) and 70% in cells incubated with 300 pM E2 for 3 d (n = 7). Apamin-sensitive currents comprised 7.6 ± 6.5% of the K(Ca) currents in cells incubated with 300 pM E2 for 3 d (n = 5). C, Voltage-protocol and example traces for I_{AHP}. The currents were activated by a 100-msec voltage pulse to +30 mV from a holding potential of −90 mV, followed by a 5-sec voltage step to −50 mV. I_{AHP} were hardly observed in cells incubated with or without E2 for 3 d. *, $P < 0.05$ *vs.* normal medium; **, $P < 0.01$ *vs.* normal medium using the Wilcoxon signed-rank test.

DPN significantly augmented the K(Ca) currents at +30, +50, and +60 mV, compared with control cells (Fig. 7A). The augmentation by DPN was observed at concentrations of 1–10 nM, but PPT in the same concentration range had no effect on K(Ca) currents (Fig. 7, A and B).
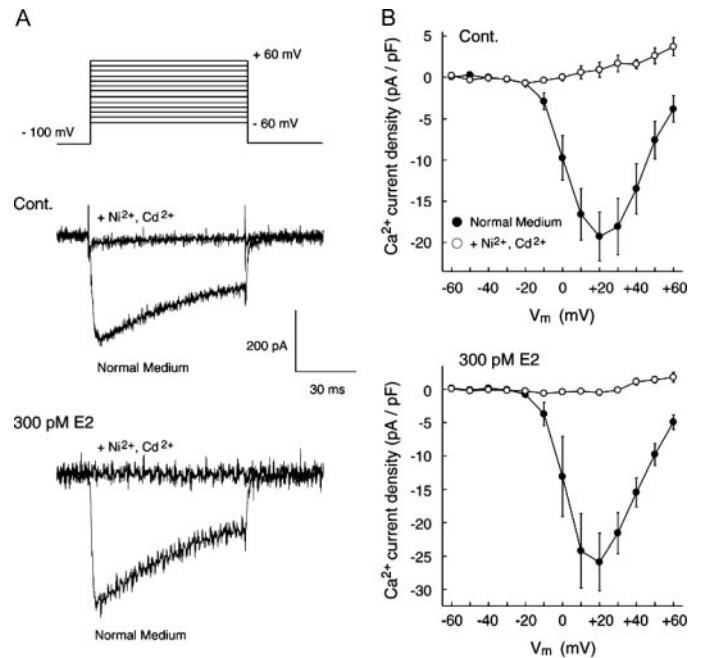

FIG. 5. Voltage-gated Ca^{2+} currents. Ca^{2+} currents were activated by 100-msec voltage pulses (−60 to +60 mV in 10-mV increments) from a holding potential of −100 mV. Example current traces activated by +20-mV voltage pulses are shown. B, Current-voltage relationship of the peak Ca^{2+} currents. There was no significant differences between the currents recorded from control cells (n = 10) and those recorded from E2-treated cells (300 pM; n = 10). Ni^{2+} and Cd^{2+} blocked the Ca^{2+} currents in the both cell groups (○).

Knockdown of ERα and ERβ

ERα and ERβ transcripts were successfully knocked down in GT1-7 cells (Fig. 8A). Preincubation with siRNA targeted to ERβ reduced the K(Ca) currents in GT1-7 cells incubated with 300 pM E2 for 3 d (Fig. 8B). By contrast, siRNA targeted to ERα failed to reduce the K(Ca) currents (Fig. 8B). Significant decreases in the K(Ca) currents in the ERβ knockdown (ERβ-KD) cells were observed at +40 to +60 mV compared with control cells, whereas the K(Ca) currents were not reduced in ERα-KD cells (Fig. 8B).

Expression of BK channel mRNAs

To examine the expression levels of BK channel subunits, RT-PCR analysis was performed on GT1-7 cells (Fig. 9). RT-PCR revealed the expression levels of four different BK channel subunits in GT1-7 cells: α-, β1-, β2-, and β4-subunits (Fig. 9A). The amplicon length for the α-subunit in the GT1-7 cells was 81 bp shorter than that in the mouse hypothalamus (26) (Fig. 9A), indicating the presence of a splice variant lacking the 23rd exon (27) in GT1-7 cells. We failed to detect the β3-subunit in GT1-7 cells (Fig. 9A). As negative controls, PCRs were performed without cDNA (− in Fig. 9A). Semi-quantitative analysis of the PCR products revealed that the levels of mRNAs for the α- and β4-subunits were significantly increased by incubating cells with 300 pM E2 for 3 d (Fig. 9B). However, E2 had no effect on the levels of mRNAs for the β1- and β2-subunits (Fig. 9B).
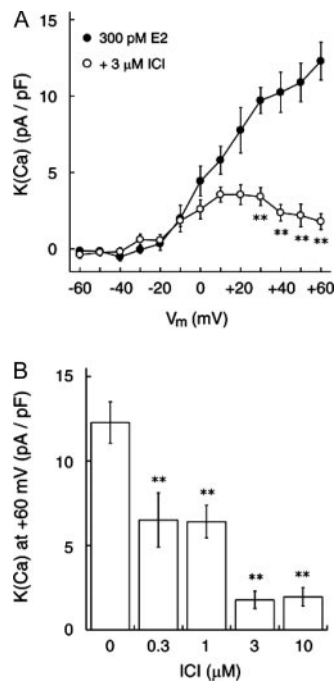
FIG. 6. The ER antagonist ICI blocked the E2-induced augmentation of the K(Ca) currents. A, Current-voltage relationships of the K(Ca) currents. The augmentation by 300 pM E2 (●, n = 10) was completely blocked by 3 μM ICI (○, n = 10). The data with 300 pM E2 alone are repeated from Fig. 3A. B, The concentration-response relationship of ICI in the presence of 300 pM E2 is shown at a voltage-pulse of +60 mV (n = 7–10). *, $P < 0.05$ *vs.* 300 pM E2 without ICI; **, $P < 0.01$ *vs.* 300 pM E2 without ICI using the Tukey-Kramer multiple comparison test.
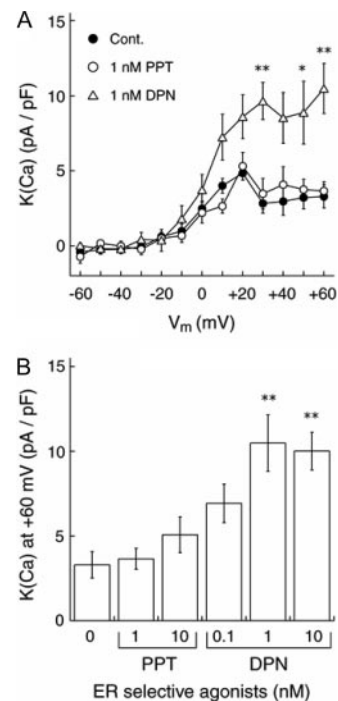

FIG. 7. Effects of selective ER agonists on the K(Ca) currents. A, The current-voltage relationships of the BK currents are collectively shown. The ERα-selective agonist PPT had no effect on K(Ca) currents (○, n = 10), whereas the ERβ-selective agonist DPN increased the BK currents at +30 mV, +50 mV and +60 mV (△, n = 10). The control data (●, n = 10) are repeated from Fig. 3A. B, Concentration-response relationships of PPT and DPN at +60 mV (n = 7–10). *, $P < 0.05$ *vs.* control; **, $P < 0.01$ *vs.* control using the Tukey-Kramer multiple comparison test.

Discussion

The present study revealed that E2 positively modulated K(Ca) currents via ERβ in GT1-7 cells. The involvement of ERβ in the augmentation of K(Ca) currents was clearly demonstrated by the following observations: 1) an ER antagonist completely blocked the response to E2 (Fig. 6); 2) a selective agonist for ERβ, but not one for ERα, mimicked this response (Fig. 7); and 3) knockdown of ERβ, but not of ERα, blocked the response (Fig. 8).

An increase in intracellular Ca^{2+} concentration ($[Ca^{2+}]_i$) is essential for the activation of K(Ca) channels. In the present experimental conditions, an increase in $[Ca^{2+}]_i$ is achieved by Ca^{2+} influx through voltage-gated Ca^{2+} channels. However, the Ca^{2+} channels are not the target of E2 action, because incubation with E2 did not augment the Ca^{2+} currents (Fig. 5).

Three types of K(Ca) currents are known (28), namely the SK currents, the intermediate-conductance K(Ca) (IK) currents, and the BK currents. Which type(s) of currents comprise the K(Ca) currents observed in the present experiments? Involvement of SK currents is unlikely, because the SK channel blocker apamin did not attenuate the K(Ca) currents, and the expression of either fast or slow after-hyperpolarization (AHP) current was very small (Fig. 4, B and C). Either current is carried through K(Ca) channels (29). Fast AHP currents in hippocampal and neocortical pyramidal neurons are carried through SK channels (30), and slow AHP currents in GnRH neurons are carried through SK channels

(31, 32). In GT1-7 cells, lack of effect of apamin on whole-cell currents induced by depolarizing voltage pulses has been reported (19), whereas apamin is reported to block the outward currents induced by mobilization of intracellular Ca^{2+}, indicating the presence of SK channels (20). The discrepancy in the effect of apamin might be due to difference in the experimental protocol. The IK currents, like the SK currents, are voltage independent and solely activated by increases in Ca^{2+} concentration. The K(Ca) currents in the control were not increased at potentials more positive than +20 mV (Fig. 3A), indicating the possible involvement of IK currents. Activation of the IK currents must be closely related to an influx of Ca^{2+} through voltage-gated Ca^{2+} channels in the present experimental conditions. The Ca^{2+}-influx reached a maximum at +10 to +20 mV and declined at more positive potentials due to a decrease in the driving force (Fig. 5). In addition, IK currents are also blocked by the BK channel blocker ChTX. Expression of IK channels in brain tumor tissues has been reported, but there are no reports of IK channel expression in normal brain tissues (33). Because GT1-7 cells are generated by genetically targeted tumorigenesis (13), these cells possibly express IK channels.

K(Ca) currents recorded from E2-treated cells increased voltage dependently (Fig. 3) and were blocked by ChTX (Fig. 4, A and B). These findings indicate that the majority of currents at potentials more positive than +20 mV are carried through BK channels, because the BK channels are dually
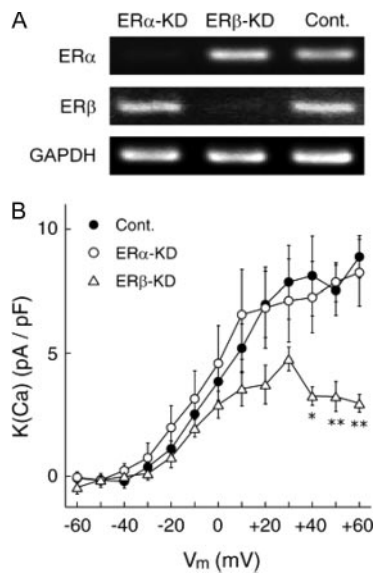
FIG. 8. Effect of ER knockdown on K(Ca) currents. Both ERα and ERβ were knocked down by siRNA. Control cells were transfected only with pCAGIPuro-EGFP, encoding enhanced green fluorescent protein. All transfected cells were cultured with 300 pM E2. A, The levels of mRNAs for the ERs were measured using RT-PCR in control (Cont.) and siRNA-treated cell groups targeted at ERα (ERα-KD) and ERβ (ERβ-KD). B, Current-voltage relationships of the K(Ca) currents. The facilitatory effect of E2 was not observed in ERβ-KD cells (△, n = 7). However, augmentation by E2 of the K(Ca) currents was observed in both ERα-KD (○, n = 7) and control cells (●, n = 7). *, $P <$ 0.05 *vs.* control; **, $P <$ 0.01 *vs.* control using the Tukey-Kramer multiple comparison test.

activated by membrane depolarization and increases in $[Ca^{2+}]_i$ (34, 35). At potentials between +20 mV and +60 mV, depolarization of the membrane potential decreases the influx of Ca^{2+}. These two interrelated factors probably cause a small increase in the activation of BK channels at these potentials. The conductance values, calculated by using the value of −90 mV as the equilibrium potential of K^+, were 0.63 pS at +20 mV and 0.74 pS at +60 mV in cells incubated with E2 and 0.39 pS at +20 mV and 0.2 pS at +60 mV in control cells. Taken together, a plausible explanation is that GT1-7 cells weakly express BK channels together with IK channels in the control condition, and incubation with E2 increases the functional expression of BK channels. Alternatively, the function of BK channels might be inhibited through an unknown mechanism, and E2 might remove this inhibition. In any case, the precise mechanism remains to be elucidated.

BK channels are composed of pore-forming α-subunits and auxiliary β-subunits (36, 37). To date, one type of α-subunit and four types of β-subunit (β1–β4) have been identified, different combinations of which form functional BK channels with different characteristics (38–42). GT1-7 cells expressed α-, β1-, β2-, and β4-subunits, similar to the expression pattern seen in the mouse hypothalamus (Fig. 9A) and rat GnRH neurons (our unpublished data). The β3-subunit, which is expressed mainly in testis, pancreas, and spleen (42), was not detected in GT1-7 cells. Blockade by ChTX was incomplete (~80%) in the present experiments (Fig. 4B). This may be due to the expression of the β4-subunit in GT1-7 cells, because coexpression of the β4-subunit with

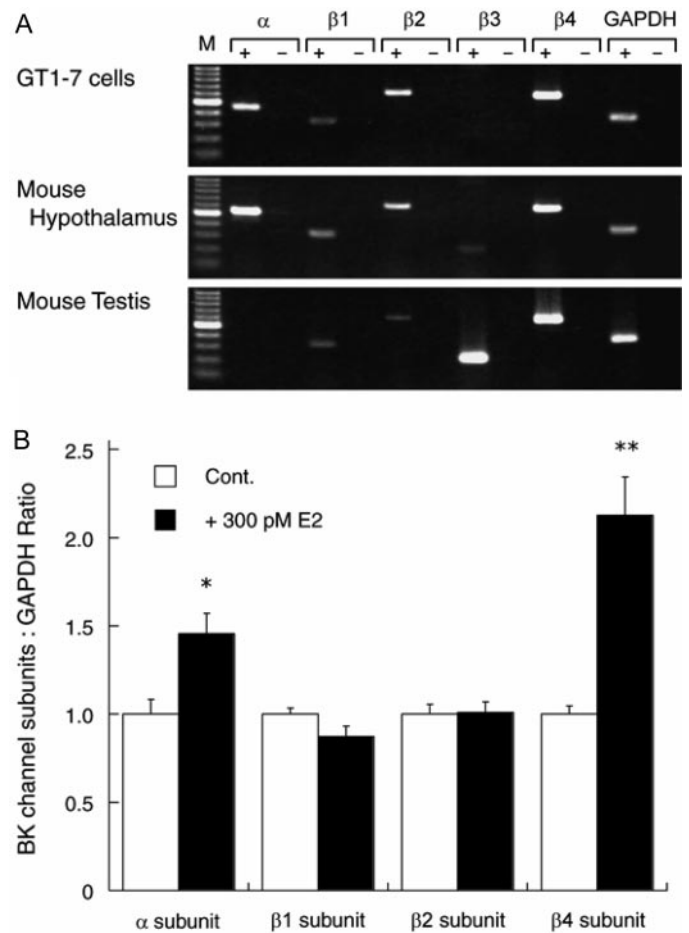FIG. 9. RT-PCR analysis of the expression of BK channel α- and β1- to β4-subunit mRNAs in GT1-7 cells. Mouse hypothalamus and testis were used as positive controls. PCRs were performed with (+) or without (−) cDNA. B, The levels of mRNAs for α- and β4-subunits in GT1-7 cells were increased by treatment with 300 pM E2 for 3 d (*black bars*, n = 7) compared with control cells (*white bars*, n = 7). However, E2 had no effect on the level of mRNAs for β1- and β2-subunits. The expression levels of each BK channel mRNA relative to the level of GAPDH mRNA in the same sample were normalized to control values. *, $P <$ 0.05 *vs.* control; **, $P <$ 0.01 *vs.* control using the *t* test.

the α-subunit in *Xenopus* oocytes reduces sensitivity to blockade by ChTX (40). Interestingly, the mRNA and proteins for the β1-subunit are increased in myometrial tissues after prolonged exposure of ovariectomized mice to E2 (43, 44), suggesting that E2 modulates BK channels at the level of transcription. The present results also demonstrated that E2 increased the level of mRNA for the α- and β4-subunits, without affecting those for the β1- and β2-subunits (Fig. 9B). An increase in the expression level of the α-subunit is likely to result in an increase in the number of BK channels. Increased expression of the β4-subunit probably attenuates the sensitivity of the channel to ChTX. These transcriptional regulations of BK channels by E2 are likely to be at least in part the cause of an increase in K(Ca) currents by E2, although the precise mechanism remains to be elucidated. The concentration-response relationship of E2 showed a bell shape with a maximal effect at 300 pM and no significant effect at 10 nM (Fig. 3B), as known for the effect of E2 on LH

secretion by rat pituitary cells (45) and uptake of dopamine into fetal rat hypothalamic cells (46).

In contrast to previous reports that demonstrated acute effects of E2 on K^+ currents (3–5), including BK currents (8, 9), we observed only a long-term effect (3 d) of E2. This difference is probably due to the concentrations of E2. We applied E2 at sub-nanomolar concentrations (Fig. 3), whereas the previous authors used E2 at nanomolar to micromolar concentrations. In rats and mice, plasma E2 levels range between a minimum of 10^{-11} M during estrus and a maximum of about 10^{-10} M during estrus (10, 11). Thus, under physiological conditions, cells are exposed to estrogens at sub-nanomolar concentrations. We did not, therefore, examine the effects of E2 at concentrations higher than this range, although locally synthesized E2 could exert acute actions at higher concentrations.

In conclusion, the present results indicate that E2 at physiological concentrations augments K(Ca) currents via ERβ, at least partly by increasing the transcription of BK channel genes, thereby modifying the excitability of GT1-7 cells. A large part of the K(Ca) currents is likely to comprise BK currents, although the possible involvement of IK currents cannot be ruled out. Finally, the present results suggest the possibility that expression of BK channels in GnRH neurons is directly regulated by E2 via ERβ, because GnRH neurons express ERβ (47–49).

Acknowledgments

References

1. **Petersen SL, Ottem EN, Carpenter CD** 2003 Direct and indirect regulation of gonadotropin-releasing hormone neurons by estradiol. Biol Reprod 69:1771–1778

2. **Watson CS, Gametchu B** 2003 Proteins of multiple classes may participate in nongenomic steroid actions. Exp Biol Med (Maywood) 228:1272–1281

3. **Nabekura J, Oomura Y, Minami T, Mizuno Y, Fukuda A** 1986 Mechanism of the rapid effect of 17 β-estradiol on medial amygdala neurons. Science 233:226–228

4. **Kelly MJ, Ronnekleiv OK, Eskay RL** 1984 Identification of estrogen-responsive LHRH neurons in the guinea pig hypothalamus. Brain Res Bull 12:399–407

5. **Minami T, Oomura Y, Nabekura J, Fukuda A** 1990 17β-Estradiol depolarization of hypothalamic neurons is mediated by cyclic AMP. Brain Res 519:301–307

6. **Abe H, Terasawa E** 2005 Firing pattern and rapid modulation of activity by estrogen in primate luteinizing hormone releasing hormone-1 neurons. Endocrinology 146:4312–4320

7. **Kow LM, Devidze N, Pataky S, Shibuya I, Pfaff DW** 2006 Acute estradiol application increases inward and decreases outward whole-cell currents of neurons in rat hypothalamic ventromedial nucleus. Brain Res 1116:1–11

8. **White RE, Han G, Maunz M, Dimitropoulou C, El-Mowafy AM, Barlow RS, Catravas JD, Snead C, Carrier GO, Zhu S, Yu X** 2002 Endothelium-independent effect of estrogen on Ca^{2+}-activated K^+ channels in human coronary artery smooth muscle cells. Cardiovasc Res 53:650–661

9. **Valverde MA, Rojas P, Amigo J, Cosmelli D, Orio P, Bahamonde MI, Mann GE, Vergara C, Latorre R** 1999 Acute activation of Maxi-K channels (*hSlo*) by estradiol binding to the β subunit. Science 285:1929–1931

10. **Smith MS, Freeman ME, Neill JD** 1975 The control of progesterone secretion during the estrous cycle and early pseudopregnancy in the rat: prolactin, gonadotropin and steroid levels associated with rescue of the corpus luteum of pseudopregnancy. Endocrinology 96:219–226

11. **Bergman MD, Schachter BS, Karelus K, Combatsiaris EP, Garcia T, Nelson JF** 1992 Up-regulation of the uterine estrogen receptor and its messenger ribonucleic acid during the mouse estrous cycle: the role of estradiol. Endocrinology 130:1923–1930

12. **DeFazio RA, Moenter SM** 2002 Estradiol feedback alters potassium currents and firing properties of gonadotropin-releasing hormone neurons. Mol Endocrinol 16:2255–2265

13. **Mellon PL, Windle JJ, Goldsmith PC, Padula CA, Roberts JL, Weiner RI** 1990 Immortalization of hypothalamic GnRH neurons by genetically targeted tumorigenesis. Neuron 5:1–10

14. **Charles AC, Hales TG** 1995 Mechanisms of spontaneous calcium oscillations and action potentials in immortalized hypothalamic (GT1-7) neurons. J Neurophysiol 73:56–64

15. **Hales TG, Sanderson MJ, Charles AC** 1994 GABA has excitatory actions on GnRH-secreting immortalized hypothalamic (GT1-7) neurons. Neuroendocrinology 59:297–308

16. **Martinez de la Escalera G, Choi AL, Weiner RI** 1994 Biphasic GABAergic regulation of GnRH secretion in GT1 cell lines. Neuroendocrinology 59:420–425

17. **Wetsel WC, Valenca MM, Merchenthaler I, Liposits Z, Lopez FJ, Weiner RI, Mellon PL, Negro-Vilar A** 1992 Intrinsic pulsatile secretory activity of immortalized luteinizing hormone-releasing hormone-secreting neurons. Proc Natl Acad Sci USA 89:4149–4153

18. **Bosma MM** 1993 Ion channel properties and episodic activity in isolated immortalized gonadotropin-releasing hormone (GnRH) neurons. J Membr Biol 136:85–96

19. **Spergel DJ, Catt KJ, Rojas E** 1996 Immortalized GnRH neurons express large-conductance calcium-activated potassium channels. Neuroendocrinology 63:101–111

20. **Van Goor F, Krsmanovic LZ, Catt KJ, Stojilkovic SS** 1999 Coordinate regulation of gonadotropin-releasing hormone neuronal firing patterns by cytosolic calcium and store depletion. Proc Natl Acad Sci USA 96:4101–4106

21. **Navarro CE, Saeed SA, Murdock C, Martinez-Fuentes AJ, Arora KK, Krsmanovic LZ, Catt KJ** 2003 Regulation of cyclic adenosine 3′,5′- monophosphate signaling and pulsatile neurosecretion by G_i-coupled plasma membrane estrogen receptors in immortalized gonadotrophin-releasing hormone neurons. Mol Endocrinol 17:1792–1804

22. **Roy D, Angelini NL, Belsham DD** 1999 Estrogen directly represses gonadotropin-releasing hormone (GnRH) gene expression in estrogen receptor-α (ERα)- and ERβ-expressing GT1-7 GnRH neurons. Endocrinology 140:5045–5053

23. **Ui-Tei K, Naito Y, Takahashi F, Haraguchi T, Ohki-Hamazaki H, Juni A, Ueda R, Saigo K** 2004 Guidelines for the selection of highly effective siRNA sequences for mammalian and chick RNA interference. Nucleic Acids Res 32:936–948

24. **Kato M, Ui-Tei K, Watanabe M, Sakuma Y** 2003 Characterization of voltage-gated calcium currents in gonadotropin-releasing hormone neurons tagged with green fluorescent protein in rats. Endocrinology 144:5118–5125

25. **Watanabe M, Sakuma Y, Kato M** 2004 High expression of the R-type voltage-gated Ca^{2+} channel and its involvement in Ca^{2+}-dependent gonadotropin-releasing hormone release in GT1-7 cells. Endocrinology 145:2375–2383

26. **Pallanck L, Ganetzky B** 1994 Cloning and characterization of human and mouse homologs of the *Drosophila* calcium-activated potassium channel gene, *slowpoke*. Hum Mol Genet 3:1239–1243

27. **Nehrke K, Quinn CC, Begenisich T** 2003 Molecular identification of Ca^{2+}-activated K^+ channels in parotid acinar cells. Am J Physiol Cell Physiol 284:C535–C546

28. **Sah P** 1996 Ca^{2+}-activated K^+ currents in neurones: types, physiological roles and modulation. Trends Neurosci 19:150–154

29. **Maylie J, Bond CT, Herson PS, Lee WS, Adelman JP** 2004 Small conductance Ca^{2+}-activated K^+ channels and calmodulin. J Physiol 554:255–261

30. **Sailer CA, Hu H, Kaufmann WA, Trieb M, Schwarzer C, Storm JF, Knaus HG** 2002 Regional differences in distribution and functional expression of small-conductance Ca^{2+}-activated K^+ channels in rat brain. J Neurosci 22:9698–9707

31. **Kato M, Tanaka N, Usui S, Sakuma Y** 2006 The SK channel blocker apamin inhibits slow afterhyperpolarization currents in rat gonadotropin-releasing hormone neurones. J Physiol 574:431–442

32. **Spergel DJ** 2007 Calcium and small-conductance calcium-activated potassium channels in gonadotropin-releasing hormone neurons before, during, and after puberty. Endocrinology 148:2383–2390

33. **Ishii TM, Silvia C, Hirschberg B, Bond CT, Adelman JP, Maylie J** 1997 A human intermediate conductance calcium-activated potassium channel. Proc Natl Acad Sci USA 94:11651–11656

34. **Pallotta BS, Magleby KL, Barrett JN** 1981 Single channel recordings of Ca^{2+}-activated K^+ currents in rat muscle cell culture. Nature 293:471–474

35. **Cui J, Cox DH, Aldrich RW** 1997 Intrinsic voltage dependence and Ca^{2+}

regulation of *mslo* large conductance Ca-activated K$^+$ channels. J Gen Physiol 109:647–673

36. **Knaus HG, Garcia-Calvo M, Kaczorowski GJ, Garcia ML** 1994 Subunit composition of the high conductance calcium-activated potassium channel from smooth muscle, a representative of the *mSlo* and *slowpoke* family of potassium channels. J Biol Chem 269:3921–3924

37. **McManus OB, Helms LM, Pallanck L, Ganetzky B, Swanson R, Leonard RJ** 1995 Functional role of the β subunit of high conductance calcium-activated potassium channels. Neuron 14:645–650

38. **Brenner R, Jegla TJ, Wickenden A, Liu Y, Aldrich RW** 2000 Cloning and functional characterization of novel large conductance calcium-activated potassium channel β subunits, hKCNMB3 and hKCNMB4. J Biol Chem 275:6453–6461

39. **Cox DH, Aldrich RW** 2000 Role of the β subunit in large-conductance Ca^{2+}-activated K$^+$ channel gating energetics. Mechanisms of enhanced Ca^{2+} sensitivity. J Gen Physiol 116:411–432

40. **Meera P, Wallner M, Toro L** 2000 A neuronal β subunit (KCNMB4) makes the large conductance, voltage- and Ca^{2+}-activated K$^+$ channel resistant to charybdotoxin and iberiotoxin. Proc Natl Acad Sci USA 97:5562–5567

41. **Xia XM, Ding JP, Lingle CJ** 1999 Molecular basis for the inactivation of Ca^{2+}- and voltage-dependent BK channels in adrenal chromaffin cells and rat insulinoma tumor cells. J Neurosci 19:5255–5264

42. **Xia XM, Ding JP, Zeng XH, Duan KL, Lingle CJ** 2000 Rectification and rapid activation at low Ca^{2+} of Ca^{2+}-activated, voltage-dependent BK currents: consequences of rapid inactivation by a novel β subunit. J Neurosci 20:4890–4903

43. **Benkusky NA, Korovkina VP, Brainard AM, England SK** 2002 Myometrial maxi-K channel β1 subunit modulation during pregnancy and after 17β-estradiol stimulation. FEBS Lett 524:97–102

44. **Nagar D, Liu XT, Rosenfeld CR** 2005 Estrogen regulates β_1-subunit expression in Ca^{2+}-activated K$^+$ channels in arteries from reproductive tissues. Am J Physiol Heart Circ Physiol 289:H1417–H1427

45. **Emons G, Ortmann O, Thiessen S, Knuppen R** 1986 Effects of estradiol and some antiestrogens (clomiphene, tamoxifen, and hydroxytamoxifen) on luteinizing hormone secretion by rat pituitary cells in culture. Arch Gynecol 237:199–211

46. **Christian M, Gillies G** 1999 Developing hypothalamic dopaminergic neurones as potential targets for environmental estrogens. J Endocrinol 160:R1–R6

47. **Hrabovszky E, Shughrue PJ, Merchenthaler I, Hajszan T, Carpenter CD, Liposits Z, Petersen SL** 2000 Detection of estrogen receptor-β messenger ribonucleic acid and ^{125}I-estrogen binding sites in luteinizing hormone-releasing hormone neurons of the rat brain. Endocrinology 141:3506–3509

48. **Hrabovszky E, Steinhauser A, Barabas K, Shughrue PJ, Petersen SL, Merchenthaler I, Liposits Z** 2001 Estrogen receptor-β immunoreactivity in luteinizing hormone-releasing hormone neurons of the rat brain. Endocrinology 142:3261–3264

49. **Kallo I, Butler JA, Barkovics-Kallo M, Goubillon ML, Coen CW** 2001 Oestrogen receptor β-immunoreactivity in gonadotropin releasing hormone-expressing neurones: regulation by oestrogen. J Neuroendocrinol 13:741–748